$Na_V1.1$ channels are critical for intercellular communication in the suprachiasmatic nucleus and for normal circadian rhythms

Sung Han[a], Frank H. Yu[b,1], Michael D. Schwartz[c,2], Jonathan D. Linton[a,d], Martha M. Bosma[a,c], James B. Hurley[a,d], William A. Catterall[a,b,3,4], and Horacio O. de la Iglesia[a,c,3,4]

[a]Program in Neurobiology and Behavior and Departments of [b]Pharmacology, [c]Biology, and [d]Biochemistry, University of Washington, Seattle, WA 98195

Edited by Jay C. Dunlap, Dartmouth Medical School, Hanover, NH, and approved December 8, 2011 (received for review September 26, 2011)

$Na_V1.1$ is the primary voltage-gated Na^+ channel in several classes of GABAergic interneurons, and its reduced activity leads to reduced excitability and decreased GABAergic tone. Here, we show that $Na_V1.1$ channels are expressed in the suprachiasmatic nucleus (SCN) of the hypothalamus. Mice carrying a heterozygous loss of function mutation in the *Scn1a* gene (*Scn1a*$^{+/-}$), which encodes the pore-forming α-subunit of the $Na_V1.1$ channel, have longer circadian period than WT mice and lack light-induced phase shifts. In contrast, *Scn1a*$^{+/-}$ mice have exaggerated light-induced negative-masking behavior and normal electroretinogram, suggesting an intact retina light response. *Scn1a*$^{+/-}$ mice show normal light induction of *c-Fos* and *mPer1* mRNA in ventral SCN but impaired gene expression responses in dorsal SCN. Electrical stimulation of the optic chiasm elicits reduced calcium transients and impaired ventro-dorsal communication in SCN neurons from *Scn1a*$^{+/-}$ mice, and this communication is barely detectable in the homozygous gene KO (*Scn1a*$^{-/-}$). Enhancement of GABAergic transmission with tiagabine plus clonazepam partially rescues the effects of deletion of $Na_V1.1$ on circadian period and phase shifting. Our report demonstrates that a specific voltage-gated Na^+ channel and its associated impairment of SCN interneuronal communication lead to major deficits in the function of the master circadian pacemaker. Heterozygous loss of $Na_V1.1$ channels is the underlying cause for severe myoclonic epilepsy of infancy; the circadian deficits that we report may contribute to sleep disorders in severe myoclonic epilepsy of infancy patients.

entrainment | neuronal oscillators | sodium channel

The mammalian suprachiasmatic nucleus (SCN) of the hypothalamus houses a master circadian clock that governs phase coordination between peripheral oscillators and overt circadian rhythms (1) as well as synchronization of these rhythms to the light–dark (LD) cycle through the retinohypothalamic tract (RHT) (2). Although SCN neurons are autonomous single-cell oscillators that rely on autoregulatory transcriptional/translational feedback loops of clock genes (3, 4), interneuronal synchronization is critical for the SCN to act as a tissue pacemaker with a coherent output (5, 6). Sodium-dependent action potentials are known to be essential for the synchronization between clock neurons in the SCN as well as necessary to maintain robust oscillations of clock gene expression (ref. 7 and reviewed in ref. 6), but the molecular identity of voltage-gated Na^+ channels contributing to the synchronization of the SCN neuronal network is currently unknown.

Over 90% of SCN neurons contain GABA as a neurotransmitter and express $GABA_A$ and $GABA_B$ receptors (8–10), and electrophysiological and pharmacological studies in vitro have pointed to GABA as a key signal mediating SCN neuronal network properties (11, 12). Studies of mutant mice show that voltage-gated sodium channel type 1 ($Na_V1.1$) encoded by the *Scn1a* gene is the primary voltage-gated Na^+ channel in several classes of GABAergic interneurons (13, 14). *Scn1a*$^{+/-}$ mice are a genetic model for a devastating form of epilepsy, severe myoclonic epilepsy of infancy (SMEI) (15–17). Loss of firing of GABAergic neurons and the resulting disinhibition of neural circuits are hypothesized to be the underlying cause of epilepsy and comorbid ataxia in this disease (13, 14, 18). Homozygous *Scn1a*$^{-/-}$ mice are more severely impaired and die on postnatal day 15 (P15) (13).

We reasoned that impairment of action potential firing and intercellular communication between SCN neurons may disrupt the function of the master circadian clock within the SCN, and therefore, our mouse model of SMEI may provide a unique opportunity to further define the role of $Na_V1.1$ channels and GABAergic neurotransmission in the SCN using a genetic approach. We report that *Scn1a*$^{+/-}$ mice have a severe disruption of their circadian system that is consistent with dramatic impairments in intercellular signaling in the SCN and can be partially rescued by pharmacological enhancement of GABAergic transmission. Our results give important insight into the critical role of the $Na_V1.1$ channel and GABAergic neurotransmission within the mammalian master circadian clock. In addition, these findings support the hypothesis that reduced excitability of the GABAergic neurons of the SCN contributes to the sleep impairment in SMEI patients.

Results

Expression of $Na_V1.1$ Channels in the SCN. We first examined expression of the $Na_V1.1$ channel in SCN neurons using in situ hybridization in brain sections from WT, *Scn1a*$^{+/-}$, and *Scn1a*$^{-/-}$ mice (13). Digoxigenin-labeled antisense oligonucleotides complementary to $Na_V1.1$ mRNA showed strong labeling in SCN neurons of WT mice but not homozygote mutant mice (Fig. 1*A*). Immunoblotting detected the $Na_V1.1$ protein in SCN tissue as a 250-kDa band with intensity that was reduced to approximately one-half of WT levels in heterozygotes [mean *Scn1a*$^{+/-}$/WT expression ratio for four experiments was 0.46; 95% confidence interval (CI) = 0.02, 0.90] and nearly zero in homozygotes (Fig. 1*B*). Expression of $Na_V1.1$ channels within SCN neurons is not

Author contributions: S.H., W.A.C., and H.O.d.l.I. designed research; S.H., M.D.S., J.D.L., M.M.B., J.B.H., W.A.C., and H.O.d.l.I. performed research; S.H., F.H.Y., M.M.B., J.B.H., and W.A.C. contributed new reagents/analytic tools; S.H., M.D.S., J.D.L., M.M.B., J.B.H., W.A.C., and H.O.d.l.I. analyzed data; and S.H., M.M.B., J.B.H., W.A.C., and H.O.d.l.I. wrote the paper.

The authors declare no conflict of interest.

This article is a PNAS Direct Submission.

[1]Present address: Program in Neurobiology, School of Dentistry and Dental Research Institute, Seoul National University, Seoul 110-749, Korea.

[2]Present address: Center for Neuroscience, Biosciences Division, SRI International, 333 Ravenswood Ave., Menlo Park, CA 94025.

[3]W.A.C. and H.O.d.l.I. contributed equally to this work.

[4]To whom correspondence may be addressed. E-mail: wcatt@uw.edu or horaciod@uw.edu.

See Author Summary on page 1840.

This article contains supporting information online at www.pnas.org/lookup/suppl/doi:10.1073/pnas.1115729109/-/DCSupplemental.

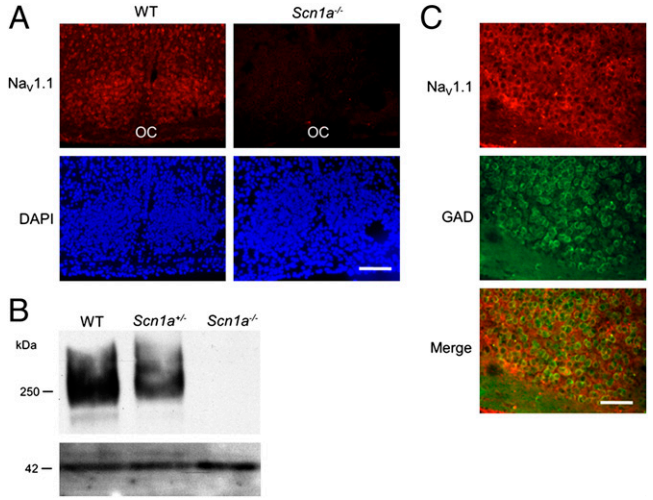

Fig. 1. $Na_V1.1$ voltage-gated Na^+ channels are expressed in SCN GABAergic cells. (*A*) Fluorescent in situ hybridization with an antisense probe against the $Na_V1.1$ mRNA labels cells in the SCN of WT mice (*Left*) but not mice homozygote for a KO mutation in the *Scn1a* gene (*Right*), which encodes the pore-forming α-subunit of the channel. *Upper* shows red immunofluorescence after antibody detection of a digoxigenin-labeled antisense riboprobe; *Lower* represents the same sections stained with DAPI. OC, optic chiasm. (*B*) Immunoblotting of SCN proteins with antibodies against the $Na_V1.1$ reveals a 250-kDa band in WT mice, a lighter band in $Scn1a^{+/-}$ mice (with one copy of the WT *Scn1a* gene), and no immunoreactivity in KO mice. The lower band shows immunoblotting of actin as a loading control. (*C*) In situ hybridization against the $Na_V1.1$ mRNA combined with GAD67 immunohistochemistry reveals expression of the channel only in GABAergic cells. *Top* shows fluorescent in situ hybridization for the *Scn1a* mRNA. *Middle* shows fluorescent immunolabeling of GAD. *Bottom* shows the merge of both fluorescence wavelengths. Eighty percent of GAD^+ cells express the channel; 100% of $Na_V1.1^+$ cells express GAD. (Scale bar: *A*, 70 μm; *B*, 35 μm.)

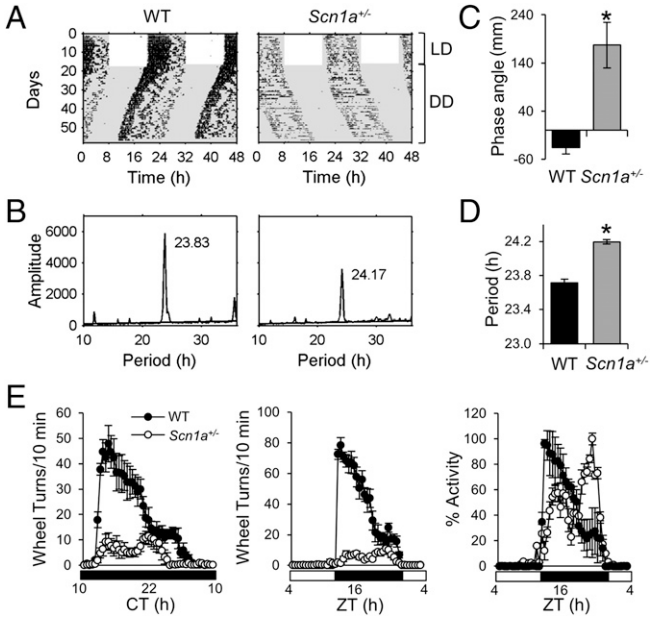

Fig. 2. Circadian behavioral phenotype in $Scn1a^{+/-}$ mice. (*A*) Wheel-running activity in representative WT and $Scn1a^{+/-}$ mice. Wheel-running activity is displayed in double-plotted actograms, with revolutions represented by black bars on vertically aligned 48-h periods. White and gray areas represent times of lights-on and darkness, respectively. (*B*) Periodogram analysis of the locomotor activity shown in *A* after transfer into constant darkness reveals a longer free-running period for the $Scn1a^{+/-}$ animal than for the WT animal. The value in hours on top of each plot indicates the period for the peak amplitude. (*C*) $Scn1a^{+/-}$ mice show a delayed phase angle of entrainment compared with WT mice. *Significantly different from WT (two-tailed Student *t* test, $P = 0.0007$, $n = 9$ for WT, $n = 10$ for $Scn1a^{+/-}$). (*D*) The period of $Scn1a^{+/-}$ animals is significantly longer than the period of WT animals. The plot shows the mean ± SEM of the values calculated by periodogram analysis. *Significantly different from WT (two-tailed Student *t* test, $P = 0.0004$, $n = 9$ for WT, $n = 10$ for $Scn1a^{+/-}$). (*E*) $Scn1a^{+/-}$ animals exhibit lower levels of activity under DD (*Left*) and LD (*Center*) conditions. During the dark phase, their activity onset is delayed relative to the WT activity onset (*Right*). Waveforms in *Left* and *Center* include 18 successive days for 9 WT (black circles) and 10 $Scn1a^{+/-}$ (white circles) mice; then, the mean ± SEM was calculated from all of the animals for each 30-min interval. *Right* shows the same data as in *Center* normalized to the maximum activity level for the 24-h period.

surprising given that this particular voltage-gated Na^+ channel plays a primary role in action potential firing in GABAergic interneurons (13), where it is expressed specifically within the neuronal soma (19), and the vast majority of SCN neurons are GABAergic (8, 9). As in previous studies (13, 14), we confirmed the expression of the $Na_V1.1$ channel within GABAergic cells (Fig. 1*C*). Cells expressing $Na_V1.1$ mRNA were more abundant within the ventral SCN, where GABAergic cells are densely packed (8), and $Na_V1.1$ expression was colocalized with immunostaining for glutamate decarboxylase (GAD), a rate-limiting enzyme for GABA synthesis (Fig. 1*C*). The number of total DAPI-stained cells did not differ between $Scn1a^{-/-}$ and WT animals (two-tailed Student *t* test, $P = 0.85$, $n = 4$ per genotype), suggesting that the mutation causes no major anatomical changes in the SCN.

Circadian Behavioral Phenotypes in $Scn1a^{+/-}$ Mice. To assess the role of $Na_V1.1$ channels in circadian behavior, we studied running-wheel activity in $Scn1a^{+/-}$ and WT mice. Both genotypes entrained to a 12:12 (LD) cycle, although the phase of activity onset of $Scn1a^{+/-}$ mice under LD conditions was delayed relative to the phase of WT mice (Fig. 2 *A*, *C*, and *E* and Fig. S1). On transfer of animals into constant darkness (DD), $Scn1a^{+/-}$ mice showed a free-running period significantly longer than the WT period (24.28 ± 0.11 vs. 23.74 ± 0.03 h, respectively; $P = 0.0004$, two-tailed Student *t* test) (Fig. 2 *A*, *B*, and *D*) and significantly longer than 24 h (95% CI = 24.02, 24.54).

The overall activity of $Scn1a^{+/-}$ mice was greatly reduced compared with WT mice under both LD and DD light conditions (Fig. 2*E*). The normalized activity profile during the dark phase was also distinct; WT mice were more active at the beginning of night, whereas $Scn1a^{+/-}$ mice were more active at the end of the night, showing a delayed activity bout (Fig. 2*E*). Overall, the amplitude of circadian locomotor activity rhythm was reduced in $Scn1a^{+/-}$ mice. Importantly, this finding was the result of both reduced activity levels during the subjective night (Fig. 2*E*) and higher activity levels during the subjective day. Of note, increased activity during the subjective day also indicates that the mild ataxic phenotype of $Scn1a^{+/-}$ mice (13) does not impair their ability to display higher levels of wheel-running activity than WT mice.

We examined the response of rhythmic locomotor activity in $Scn1a^{+/-}$ mice to a phase-shifting light pulse. A brief light pulse applied during the early subjective night is associated with a delay in the circadian pacemaker (20–22). WT mice showed a 2.8 h mean phase delay in wheel-running activity in response to a 30-min, 500-lux light pulse applied at circadian time 16 (CT16, with CT12 corresponding to the onset of locomotor activity) (Fig. 3 *A* and *B*). This delay was statistically different from zero (95% CI = −4.8, −0.8). In contrast, $Scn1a^{+/-}$ mice failed to respond to the same light treatment (Fig. 3 *A* and *B*) (mean = 0.4 h, 95% C = −1.4, 2.2).

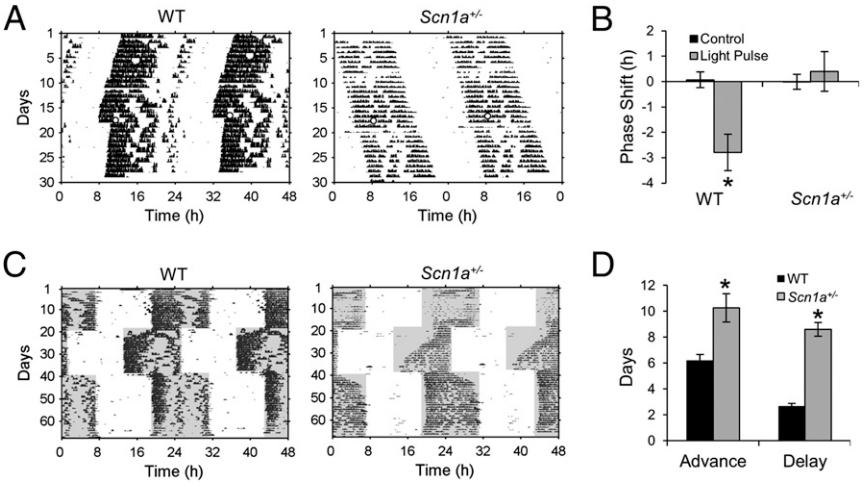

Fig. 3. Impaired circadian photoresponsiveness in *Scn1a*$^{+/-}$ mice. (*A*) *Scn1a*$^{+/-}$ mice fail to respond with a delay to a 30-min light pulse applied during the early subjective night. Representative actograms of WT and *Scn1a*$^{+/-}$ animals that received a 30-min, 500-lux light pulse starting at CT16 (white circle) and showed a delay or no response, respectively. (*B*) Light pulses at CT16 induced delays in WT but not *Scn1a*$^{+/-}$ mice. Values represent mean ± SEM for control dark- and light-pulsed animals. *Only group that showed a mean shift with 95% CI that did not include zero (n = 4 and 5 for WT control and light pulse, respectively; n = 5 and 8 for *Scn1a*$^{+/-}$). (*C*) *Scn1a*$^{+/-}$ mice exhibit slower reentrainment to abrupt phase shifts of the LD cycle than WT mice. Representative actograms of WT and *Scn1a*$^{+/-}$ animals exposed to an abrupt 6-h advance and later, to an abrupt 6-h delay. (*D*) The number of days to achieve full reentrainment is longer for *Scn1a*$^{+/-}$ than WT mice both for delays and advances (n = 6 and 6 for WT mice for advances and delays, respectively; n = 12 and 10 for *Scn1a*$^{+/-}$ mice). Values represent mean ± SEM. *Statistically different from WT mice (two-way ANOVA, significant effect of genotype, $P < 0.0001$).

Impairment in photic phase resetting in *Scn1a*$^{+/-}$ mice was also evident after exposing animals to abrupt phase shifts of the LD cycle. After a 6-h delay, it took 8.6 ± 0.5 d for *Scn1a*$^{+/-}$ mice to fully reentrain compared with 2.7 ± 0.2 d for WT (Fig. 3 *C* and *D*). This slow reentrainment of *Scn1a*$^{+/-}$ mice was also evident for advances of the LD cycle (10.2 ± 1.1 d for *Scn1a*$^{+/-}$ mice; 5.7 ± 0.9 d for WT mice) (Fig. 3 *C* and *D*). A two-way ANOVA revealed an effect of genotype ($P < 0.0001$) and an effect of the shift type (delay vs. advance, $P = 0.01$) but no effect of the interaction ($P = 0.34$). Thus, *Scn1a*$^{+/-}$ mice have impaired circadian photoresponsiveness, which is evident as a lack of response to nocturnal light pulses and a significantly slower reentrainment after abrupt phase shifts mimicking jetlag.

***Scn1a*$^{+/-}$ Mice Show Exaggerated Negative Masking Behavior and Normal Electroretinography.** As shown in Fig. 3, *Scn1a*$^{+/-}$ mice failed to respond to a phase-resetting light pulse during the early subjective night and showed a significantly impaired response to abrupt phase shifts of the LD cycle. This overall impairment of circadian photoresponsiveness could reflect a failure of the retina to relay light information to the SCN. To test this hypothesis, we examined the ability of light to inhibit nocturnal wheel running, known as negative masking (23), a response that is usually associated with normal photoentrainment of circadian rhythms (2). We delivered a 4-h light pulse of different intensity during the early night [Zeitgeber time (ZT) 15 to ZT19, with ZT12 being the time of lights off) and measured the percent inhibition of wheel-running activity relative to the activity at the same time on the following day when light was not presented during the night (Fig. 4*A*). As expected, WT mice showed moderate positive masking (increased wheel-running activity) under dim (2 lux) red light and negative masking that was progressively stronger with increasing white light intensity (Fig. 4*B*). Remarkably, *Scn1a*$^{+/-}$ mice did not show positive masking under 2-lux red light; instead, their activity was inhibited significantly more than in WT animals under the same intensity. Furthermore, *Scn1a*$^{+/-}$ mice showed stronger negative masking across light intensities (Fig. 4 *A* and *B*) [two-way ANOVA, significant effect of light intensity ($P < 0.0001$), genotype ($P < 0.0001$), and interaction ($P < 0.0001$)].

We also measured electroretinography (ERG) for *Scn1a*$^{+/-}$ and WT mice to test for a possible retinal abnormality. Analysis of electroretinograms showed no significant difference in the a-wave amplitude (two-tailed Student t test, $P = 0.26$), b-wave amplitude (two-tailed Student t test, $P = 0.26$), or a-wave width (WT, 18.44 ± 0.63; *Scn1a*$^{+/-}$, 17.5 ± 1.42; two-tailed Student t test, $P = 0.56$) between the two genotypes (Fig. 4 *C* and *D*). Thus, we found no evidence for a defect in the outer retina that could explain the paradoxical presence of increased negative masking—a form of nonimage-forming photoreception that is usually affected in parallel to circadian photoreception—and the failure of light to induce phase shifts in *Scn1a*$^{+/-}$ mice.

Clock Gene Expression Pattern in *Scn1a*$^{+/-}$ Mice. Autoregulatory transcriptional/translational feedback loops of clock genes constitute the molecular clockwork of single-cell circadian oscillators (4). Abnormal circadian rhythmicity in *Scn1a*$^{+/-}$ mice could be caused by altered clock gene expression within the SCN. The expression of the clock genes *Per1* and *Per2* oscillates with a peak during the day or subjective day; the peak of *Per2* mRNA slightly lags the peak of *Per1* (24–26). We examined the circadian expression pattern of *Per1* and *Per2* mRNA by in situ hybridization in WT and *Scn1a*$^{+/-}$ brain slices from animals killed every 4 h after at least 24 h under DD. *Per1* mRNA was rhythmic for both genotypes, with a peak between CT4 and CT8 (Fig. 5 *A* and *B*). A two-way ANOVA yielded a significant effect of time ($P < 0.0001$), genotype ($P = 0.035$), and interaction ($P = 0.001$). The mRNA levels oscillated with slightly lower amplitude in *Scn1a*$^{+/-}$ than WT mice. *Per2* expression levels also followed a similar circadian expression pattern but with an approximate 4-h delay relative to *Per1* (Fig. 5 *C* and *D*). A two-way ANOVA revealed no effect of genotype ($P = 0.16$) but a significant effect of time ($P < 0.0001$) and interaction ($P = 0.04$), which was also a consequence of a slightly lower amplitude oscillation in *Scn1a*$^{+/-}$ mice. Thus, although the expression of both clock genes oscillates with the normal phase in *Scn1a*$^{+/-}$ mice, their oscillation shows lower amplitude.

***Scn1a*$^{+/-}$ Mice Show Decreased Signal Propagation from Ventral to Dorsal SCN After Photic Stimulation.** The impaired photic responses of the circadian system of *Scn1a*$^{+/-}$ mice contrast with the in-

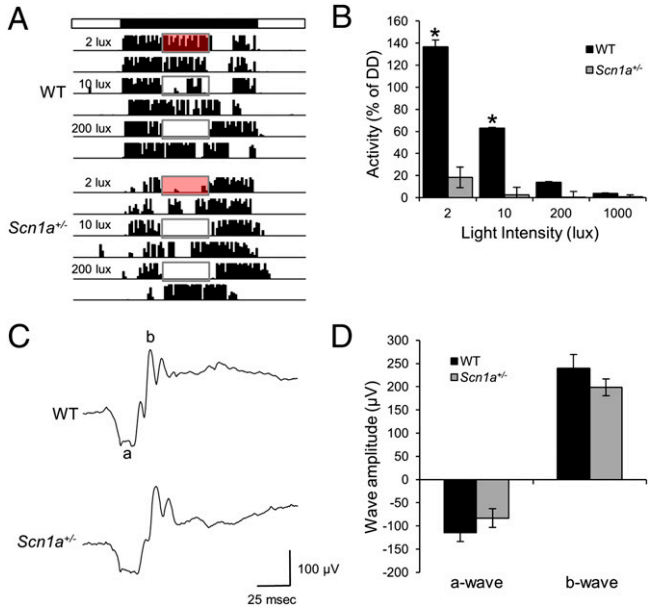

Fig. 4. *Scn1a*$^{+/-}$ mice show negative masking and normal ERG. (*A*) Nocturnal light produces stronger inhibition of activity in *Scn1a*$^{+/-}$ than WT mice. Representative actograms of WT and *Scn1a*$^{+/-}$ mice that were exposed to 4-h light pulses of 2-lux red light, 10-lux white light, and 200-lux white light in the middle of the night. The top bar represents the time of lights on (white) and off (black). Red or white rectangles represent the time in which lights were turned on in the middle of the night. Negative masking by light is evident as inhibition of nocturnal wheel-running. (*B*) *Scn1a*$^{+/-}$ mice exhibit stronger negative masking than WT mice. Values represent the percent inhibition calculated as the percent of activity that remained under each light intensity relative to the activity in the absence of light on the next day at the same ZT. *Statistically significant difference between genotypes (Tukey contrasts, $P = 0.05$; $n = 12$ for WT, $n = 9$ for *Scn1a*$^{+/-}$ mice). (*C*) Representative electroretinographic traces induced by a single flash (1.5 log cd × s/m^2) in WT and *Scn1a*$^{+/-}$ mice. (*D*) Quantification of dark-adapted a- and b-waves led to no statistical differences between genotypes ($n = 8$ for each genotype).

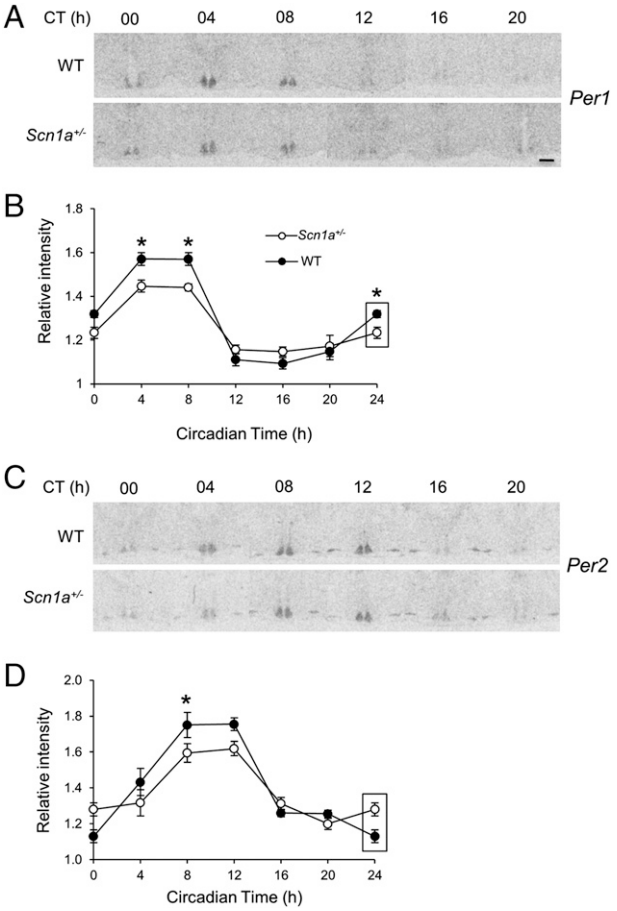

Fig. 5. Circadian clock gene expression in *Scn1a*$^{+/-}$ mice. (*A*) Representative autoradiographs of SCN sections from WT and *Scn1a*$^{+/-}$ animals killed at different circadian times and hybridized with an antisense radiolabeled probe against *Per1* mRNA. (Scale bar: 140 µm.) (*B*) Normalized optical densities from WT and *Scn1a*$^{+/-}$ animals show that the levels of *Per1* oscillate in mice of both genotypes with the same phase but with lower amplitude in *Scn1a*$^{+/-}$ mice. Values represent mean ± SEM. Two-way ANOVA: significant effect of time ($P < 0.0001$), genotype ($P = 0.035$), and interaction ($P = 0.001$). *Significant difference between genotypes for that specific time point (Student *t* test contrasts, $P = 0.05$). (*C* and *D*) Same as in *A* and *B*, but sections were hybridized with an antisense radiolabeled probe against *Per2* mRNA. Two-way ANOVA: no effect of genotype ($P = 0.16$) but significant effect of time ($P < 0.0001$) and interaction ($P = 0.04$). Rectangles on values in *B* and *D* label CT0 values that are replotted for easier visualization of the oscillation. For *B* and *D*, *n* is at least six animals per genotype and time point.

creased negative masking of their nocturnal activity and suggest that the failure of light pulses to induce phase shifts during the subjective night may reflect an inability of the SCN to decode retinal afferent input. Photic information to the circadian system is relayed by retinal ganglion cells that innervate the SCN through the RHT (2). In the mouse, RHT fibers innervate predominantly the ventral SCN, and light pulses during the subjective night, but not during the subjective day, acutely induce the expression of the immediate-early gene *c-Fos* and the clock gene *Per1* (27, 28). This induction of gene expression takes place initially within the ventral SCN and later propagates to the dorsal SCN (28–32). Because the photic induction of both behavioral phase shifts and *Per1* expression is restricted to the night, the acute induction of clock gene expression by light is thought to be critical for phase resetting of the clock. We therefore examined the light-induced gene expression pattern in WT and *Scn1a*$^{+/-}$ mice. Animals maintained under DD were killed 0, 15, 30, 60, and 90 min after the onset of a 30-min, 500-lux light pulse that started at CT16. Brains were collected and SCN slices were processed for in situ hybridization for *c-Fos* or *Per1* mRNA. Fig. 6*A* shows that *c-Fos* expression was initiated early (15 min) after the light pulse, reached a peak at 30 min, and decreased thereafter in both WT and *Scn1a*$^{+/-}$ SCN. Light-induced expression of *c-Fos* initially started in the ventral SCN with moderately higher levels in WT animals (Fig. 6 *A* and *B*) [two-way ANOVA, significant effect of genotype ($P < 0.0001$), time ($P < 0.0001$), and interaction ($P = 0.02$)]. In *Scn1a*$^{+/-}$ SCN, *c-Fos* expression was more confined to the ventral SCN, and its propagation to the dorsal SCN was much less prominent 30 min after the onset of the light pulse (Fig. 6 *A* and *B*) [two-way ANOVA, significant effect of genotype ($P < 0.0001$), time ($P < 0.0001$), and interaction ($P = 0.0001$)].

The increase in *Per1* expression was more gradual than the increase in *c-Fos* expression. Within the ventral SCN, the increase of *Per1* mRNA was similar between WT and *Scn1a*$^{+/-}$ mice (Fig. 6 *C* and *D*) [two-way ANOVA, no effect of genotype ($P = 0.13$) and a significant effect of time ($P < 0.0001$) and interaction ($P = 0.03$)], with reduced expression in *Scn1a*$^{+/-}$ animals only after 60 min. In contrast to the expression of *Per1* in the ventral SCN, its expression was substantially decreased in the dorsal SCN of *Scn1a*$^{+/-}$ mice (Fig. 6 *C* and *D*) [two-way ANOVA, significant effect of genotype ($P = 0.0001$), time ($P < 0.0001$), and interaction ($P = 0.0006$)], with significantly lower expression levels than in WT mice for every time point after light stimulation. Thus, the analysis of light-induced expression of

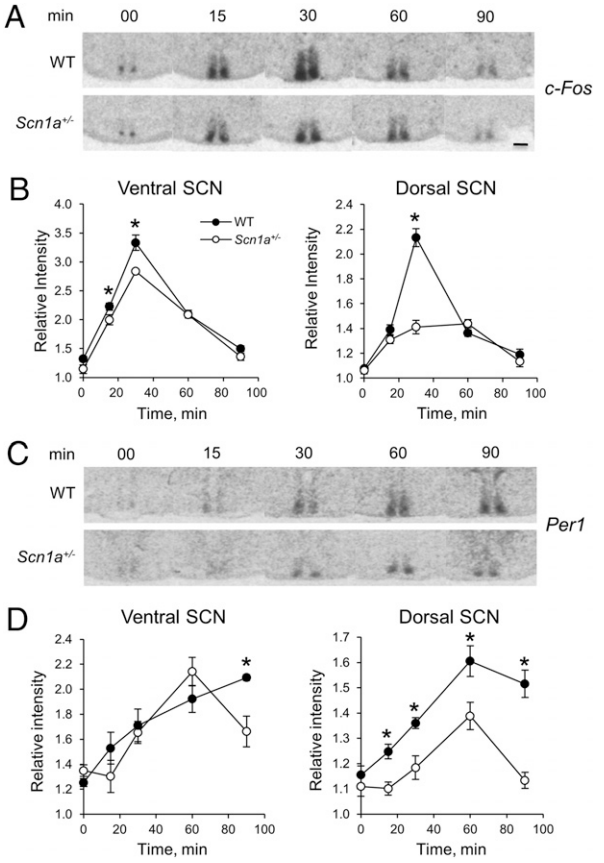

Fig. 6. *Scn1a*$^{+/-}$ mice show decreased signal propagation from ventral to dorsal SCN after photic stimulation. (*A*) Representative autoradiographs of SCN sections from WT and *Scn1a*$^{+/-}$ animals killed at different times after the onset of a 30-min, 500-lux light pulse starting at CT16 (time 0) and hybridized with an antisense radiolabeled probe against *c-Fos* mRNA. (*B*) Relative *c-Fos* mRNA expression within the ventral and dorsal SCNs at different times after light pulse onset. Two-way ANOVA for ventral: significant effect of genotype ($P < 0.0001$), time ($P < 0.0001$), and interaction ($P = 0.02$). Two-way ANOVA for dorsal: significant effect of genotype ($P < 0.0001$), time ($P < 0.0001$), and interaction ($P = 0.0001$). (*C* and *D*) Same as *A* and *B*, but sections were hybridized with an antisense radiolabeled probe against *Per1* mRNA. Two-way ANOVA for ventral: no effect of genotype ($P = 0.13$) but significant effect of time ($P < 0.0001$) and interaction ($P = 0.03$). Two-way ANOVA for dorsal: significant effect of genotype ($P = 0.0001$), time ($P < 0.0001$), and interaction ($P = 0.0006$). For *B* and *D*, $n = 6$ per genotype and time point. *Statistically significant difference between genotypes (Student *t* test contrasts, $P = 0.05$).

c-Fos and particularly, the clock gene *Per1* in the *Scn1a*$^{+/-}$ mouse reveals a rather normal response in the ventral SCN but an impaired response in the dorsal SCN, consistent with impairment of the ability of the ventral SCN to relay photic information to the dorsal SCN.

***Scn1a*$^{+/-}$ Mice Show Reduced SCN Signal Propagation from Ventral to Dorsal SCN After in Vitro RHT Stimulation.** Retinal ganglion cells innervate the SCN, and both in vivo and in vitro experiments have shown a preeminent role of glutamate, released by these RHT fibers, in transducing photic information to entrain the clock (2, 33). Light induces the synaptic release of glutamate, which activates AMPA and NMDA receptors in the ventral SCN, leading to increases in intracellular Ca^{2+} ($[Ca^{2+}]_i$) that are key to phase resetting of the molecular clockwork (34). In turn, ventral SCN neurons convey photic information to neurons in the dorsal SCN. The effect of light and glutamate release can be mimicked by the stimulation of RHT fibers in hypothalamic slices containing the SCN and the optic chiasm. Electrical stimulation of the chiasm induces increases in $[Ca^{2+}]_i$, and these increases are dependent on the occurrence of postsynaptic action potentials (35). $Na_V1.1$ is the primary sodium channel in the cell bodies of several classes of GABAergic interneurons, and its reduced activity results in decreased excitability of these cells after postsynaptic depolarization (13, 14). We reasoned that this reduced excitability could lead to smaller increases in $[Ca^{2+}]_i$ within ventral SCN neurons and reduced propagation of the signal into dorsal neurons after RHT stimulation. We incubated coronal SCN slices from WT, *Scn1a*$^{+/-}$, and *Scn1a*$^{-/-}$ P14 mice with the membrane-permeable calcium indicator dye fluo-4/AM, which allows monitoring of single-cell activity simultaneously in multiple neurons. RHT stimulation of WT SCN slices with stimulation frequencies within the physiological range of firing of retinal ganglion cells that innervate the SCN (36) (0.1–20 Hz) led to increased $[Ca^{2+}]_i$ in SCN neurons that was dependent on stimulation frequency as previously reported (35) (Fig. 7 *A* and *B*). These increases occurred first in ventral SCN neurons and later, with lower amplitude, in dorsal cells (Fig. 7 *C* and *D*). Whereas in WT SCN, 10-Hz stimulation resulted in robust increases of $[Ca^{2+}]_i$ in both ventral and dorsal SCN neurons, these increases were reduced to 50% and 30% of WT values in *Scn1a*$^{+/-}$ and *Scn1a*$^{-/-}$ mice, respectively (Fig. 7 *C* and *D*). The peak intensity ratios of the dorsal over ventral $[Ca^{2+}]_i$ increases in the *Scn1a*$^{+/-}$ and *Scn1a*$^{-/-}$ were significantly lower than the ratio of WT (Fig. 7*E*) [one-way ANOVA, significant effect of genotype ($P = 0.01$)]. A two-way ANOVA of the latency of cells to show peak fluorescence revealed a significant effect of genotype ($P = 0.0024$) and region ($P = 0.04$) and no effect of the

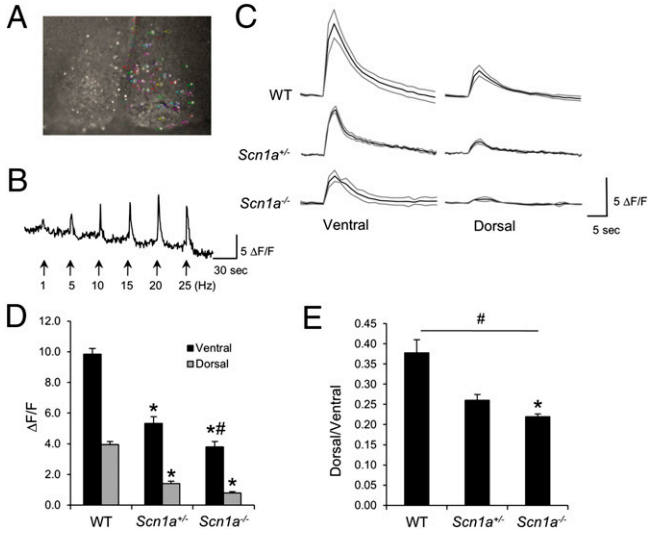

Fig. 7. *Scn1a*$^{+/-}$ mice show reduced SCN neuronal excitability and signal propagation from ventral to dorsal SCN after in vitro RHT stimulation. (*A*) Fluorescent photomicrograph of an SCN slice after incubation with the Ca^{2+}-sensitive dye fluo-4/AM and stimulation of the optic chiasm. Fluorescent single cells are circled with different colors. (*B*) $[Ca^{2+}]_i$ increase in a single cell is proportional to stimulation frequency. (*C*) Average single-cell $[Ca^{2+}]_i$ increases after optic chiasm stimulation in SCN slices from WT, *Scn1a*$^{+/-}$, and *Scn1a*$^{-/-}$ mice. (*D*) $[Ca^{2+}]_i$ increases are significantly lower in *Scn1a*$^{+/-}$ and *Scn1a*$^{-/-}$ SCN cells than WT SCN cells. *Significantly different from WT in the same region (Tukey contrasts, $P = 0.05$). #Significantly different from *Scn1a*$^{+/-}$ in the same region (Tukey contrasts, $P = 0.05$). (*E*) Signal propagation from ventral to dorsal SCN measured as the ratio of $[Ca^{2+}]_i$ increase between cells in each region is reduced in *Scn1a*$^{+/-}$ and KO mice. #Main effect of genotype ($P = 0.01$, one-way ANOVA). *Significantly different from WT (Tukey contrasts, $P = 0.05$); $n = 6$ for WT, $n = 4$ for *Scn1a*$^{+/-}$, and $n = 4$ for *Scn1a*$^{-/-}$ mice.

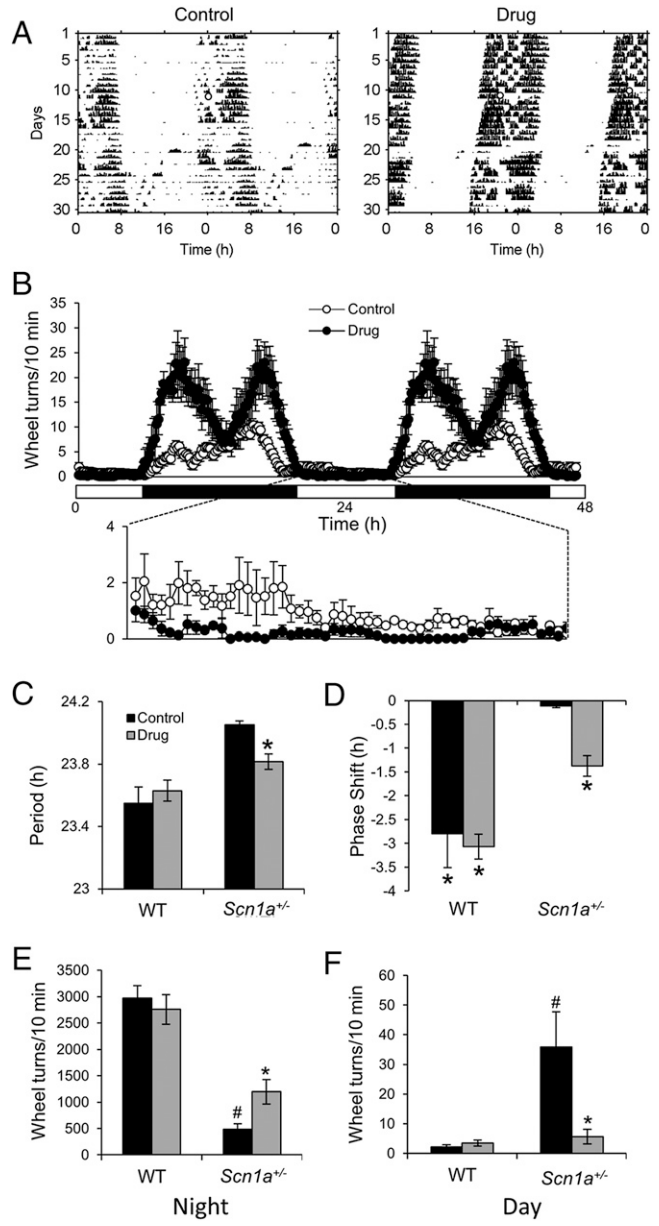

Fig. 8. Treatment with drugs that enhance GABAergic neurotransmission partially rescues the circadian phenotype of *Scn1a*$^{+/-}$ mice. (*A*) Representative actograms of a control *Scn1a*$^{+/-}$ mouse and an *Scn1a*$^{+/-}$ mouse treated with a mixture of tiagabine (2.5 mg/kg) and clonazepam (1 mg/kg) (drug) under DD and then exposed to a light pulse at CT16 (white circle). (*B*) GABAergic transmission enhancement rescues nocturnal activity levels and the distribution of nocturnal activity to a more consolidated onset at the time of lights off. It also decreases diurnal activity. Waveforms include 18 successive days for four drug-treated (black circles) and three control (white circles) *Scn1a*$^{+/-}$ mice; then, the mean ± SEM was plotted from all of the animals for each 10-min interval. (*C*) Drug treatment shortens the period of *Scn1a*$^{+/-}$ mice but not WT mice. *Significantly different from control (P = 0.01, two-tailed Student t test; n = 5 for each WT group, n = 3 for control mice, and n = 4 for drug-treated *Scn1a*$^{+/-}$ mice). (*D*) Drug treatment rescues the inability of *Scn1a*$^{+/-}$ mice to show phase delays in response to light pulse at CT16. *Groups that showed a mean shift with 95% CI that did not include zero (n = 5 for each WT group, n = 3 for control mice, n = 4 for drug-treated *Scn1a*$^{+/-}$). (*E* and *F*) Drug treatment increases nocturnal activity and decreases diurnal activity in *Scn1a*$^{+/-}$ mice but not WT mice. Bars represent the 12-h (day or night) mean ± SEM of running-wheel activity during 20 d. *Significantly different from control (planned least-squares comparisons, P = 0.02 for night and P = 0.0003 for day). #Significantly different from WT control (planned least-squares comparisons, $P < 0.0001$ for night and day); n = *5 for both WT groups,* n = *3 for control group, and* n = *4 for drug-treated* Scn1a$^{+/-}$ *group.*

interaction (P = 0.15), with an increased latency for *Scn1a*$^{-/-}$ and *Scn1a*$^{+/-}$ cells compared with WT cells (Tukey contrasts, P = 0.05). These data, along with our in situ hybridization data, indicate that the signal transmission between ventral and dorsal SCNs in the *Scn1a*$^{+/-}$ and *Scn1a*$^{-/-}$ is significantly reduced as a consequence of loss of $Na_V1.1$ activity.

Treatment with Drugs That Enhance GABAergic Neurotransmission Partially Rescues the Circadian Phenotype of *Scn1a*$^{+/-}$ Mice. In Fig. 1, we show that the $Na_V1.1$ channels are expressed in the GABA-containing SCN neurons. Furthermore, reduced $Na_V1.1$ activity is known to drastically reduce the excitability of GABAergic interneurons in both the hippocampus (13) and cerebellum (14). Therefore, we hypothesized that the circadian phenotype in the *Scn1a*$^{+/-}$ mice may be caused by reduced GABAergic transmission as a consequence of decreased $Na_V1.1$ activity in the SCN. To test this hypothesis, we treated mice with tiagabine, a GABA reuptake blocker (2.5 mg/kg), and clonazepam, an allosteric modulator of the $GABA_A$ receptor (1 mg/kg) by adding both drugs to the rodent diet (BIO-SERV). These food doses result in ∼0.4 and 0.16 mg/kg adult body weight per day of tiagabine and clonazepam, respectively (37). We provided the GABAergic transmission-enhancing drugs from P1 by supplying the food pellets to lactating mothers. Animals treated with this drug combination throughout their lifespan and untreated control animals were tested by measurement of wheel-running activity. Drug treatment had no effect on WT mice but significantly rescued the impaired circadian behavior of *Scn1a*$^{+/-}$ mice (Fig. 8). The long circadian period of *Scn1a*$^{+/-}$ mice (τ = 24.05 ± 0.02 h) was significantly shortened (τ = 23.8 ± 0.05 h, P = 0.01) (Fig. 8*C*). Light-induced phase delays in the *Scn1a*$^{+/-}$ mice were also significantly increased from −0.11 ± 0.036 to −1.37 ± 0.21 h (P = 0.05) (Fig. 8*D*). Drug treatment led to a rescue of circadian amplitude as well, which was evident as increased nocturnal activity and decreased diurnal activity (Fig. 8 *B*, *E*, and *F*). The drug-increased nocturnal activity in *Scn1a*$^{+/-}$ mice was bimodal and had a different profile than the activity of WT animals (compare Fig. 8*B* with Fig. 2*E*). A two-way ANOVA for light phase activity led to a significant effect of genotype (P = 0.0009), drug treatment (P = 0.0036), and interaction (P = 0.0019), and planned least-squares comparisons showed that GABAergic transmission enhancement decreased diurnal activity in *Scn1a*$^{+/-}$ but not WT mice (Fig. 8*F*). A two-way ANOVA for dark phase activity led to a significant effect of genotype ($P < 0.0001$), no effect of drug treatment (P = 0.17), and a significant effect of interaction (P = 0.017); planned least-squares comparisons showed that GABAergic transmission enhancement increased nocturnal activity in *Scn1a*$^{+/-}$ but not WT mice (Fig. 8*E*). Importantly, the doses of tiagabine and clonazepam used do not induce sedative effects, which is consistent with the increased nocturnal activity that we observed in drug-treated *Scn1a*$^{+/-}$ mice. Taken together, these data show that the circadian abnormality of *Scn1a*$^{+/-}$ mice is, at least in large part, because of the decreased GABAergic transmission in the SCN as a consequence of decreased $Na_V1.1$ channel function.

Discussion

Our results show that heterozygous loss-of-function mutation of the $Na_V1.1$ channel in mice leads to major circadian abnormalities, including a longer circadian period, decreased circadian amplitude, delayed activity onset, and severely impaired circadian photoresponsiveness compared with WT mice. Our study

assessed the effect of the reduced activity of a specific voltage-gated Na^+ channel in the SCN neuronal network. The significant recovery of all circadian defects in *Scn1a*$^{+/-}$ mice by GABAergic transmission-enhancing drugs points to decreased GABAergic transmission within the SCN—because of reduced $Na_V1.1$ channel activity—as the main cause for this disrupted circadian phenotype.

Although an increase of the WT period by 0.5 h in *Scn1a*$^{+/-}$ mice seems moderate, it is remarkable for a heterozygous mutation of a nonclock gene, because changes of comparable magnitude are observed in heterozygous mutations of core clock components, such as the gene *Clock* (38). Furthermore, a change from a circadian period shorter than 24 h to one longer than 24 h has dramatic effects on the phase angle of entrainment (21); thus, the longer circadian period of *Scn1a*$^{+/-}$ mice is predictive of the delay of several hours in their locomotor activity, which is clearly the case in *Scn1a*$^{+/-}$ mice. Children with SMEI have impaired sleep–wake cycles, including delayed sleep onset and difficulty maintaining sleep (39). The delayed phase of entrainment may, in part, explain delayed sleep onset in SMEI patients, because a delayed phase would push the time of sleep onset to a later time in the day. A similar effect of a change in circadian period, although in the opposite direction, seems to be responsible for familial advanced sleep phase syndrome (40, 41).

The circadian oscillation in clock gene expression that we report in *Scn1a*$^{+/-}$ mice has moderately lower amplitude than the oscillation in WT mice, suggesting that a lower-amplitude master circadian clock is, in part, responsible for their lower amplitude behavioral rhythm. The difficulty to maintain sleep reported in SMEI patients could, in part, emerge from a lower circadian amplitude oscillator that fails to sustain sleep during the night and/or wakefulness during the day.

***Scn1a*$^{+/-}$ Mice Have Impaired Function of Their Master Circadian Clock.** The widespread expression of $Na_V1.1$ channels in SCN neurons and the extent of impairment of clock function in *Scn1a*$^{+/-}$ mice point to a critical role of $Na_V1.1$ channels in the mammalian master circadian clock. The heterozygous *Scn1a*$^{+/-}$ mice have a circadian period that is significantly longer than the WT period and also longer than 24 h. Their activity during subjective night is markedly shifted to the end of the dark period. Remarkably, they have completely lost the ability to shift the phase of their circadian clock in response to a strong delaying light pulse, and their resynchronization speed after an abrupt shift in the LD cycle is profoundly reduced. Altogether, these deficits, and particularly, the changes in circadian period, indicate that reduced $Na_V1.1$ activity directly impairs SCN function.

Recent studies have shown that the long photoperiod scattering of circadian phases of single-cell neuronal oscillators in the SCN is associated with a low-amplitude electrical activity rhythm in the SCN tissue as a whole (42, 43), suggesting that the lower amplitude circadian rhythms in *Scn1a*$^{+/-}$ mice may result from uncoupling of SCN neurons caused by reduced $Na_V1.1$ channel activity. If this suggestion is the case, the reduced amplitude of *Per1* and *Per2* expression in *Scn1a*$^{+/-}$ mice may reflect a population of neurons that are oscillating with scattered phases rather than a reduction of clock gene oscillation amplitude within each cell. This interpretation is consistent with the finding that TTX applied to hypothalamic slices blocks SCN action potentials but does not affect the circadian oscillation of clock genes (44), although longer-term TTX blockade may interfere with clock gene expression (7). Similarly, circadian clock gene expression does not seem to be impaired in animals with reduced delayed rectifier potassium currents (45) or aged animals (46), both of which show low-amplitude circadian rhythms. Finally, decreased amplitude of circadian locomotor activity could also result from the reduced $Na_V1.1$ channel activity in brain regions outside of the SCN.

The lack of light-induced phase shift in *Scn1a*$^{+/-}$ mice is likely caused at the level of the SCN, because there is no deficit in light-induced negative masking or the ability of light to induce clock gene expression within the ventral SCN. Although reduced photic phase shifting would not be predicted for a low-amplitude oscillator (21), recent studies have shown that scattering of the phases of single-cell neuronal oscillators in the SCN results both in low-amplitude circadian rhythms and reduced phase-shifting ability (42). Thus, our results suggest that reduced $Na_V1.1$ activity within the SCN neuronal network may account for both the low amplitude circadian rhythms and a reduced ability to respond to phase-shifting light stimuli. Our negative masking experiments show that *Scn1a*$^{+/-}$ mice are more sensitive to light than WT mice. Genetic mutations that affect retinal sensitivity usually cause both reduced light-induced phase shifts and diminished negative masking (47, 48). Our results show that circadian photoresponsiveness and negative masking can be affected in opposite directions in an animal with intact retinal photoreception. Although our study does not exclude a retinal abnormality in layers other than the outer retina in *Scn1a*$^{+/-}$ mice (e.g., intrinsically photoreceptive ganglion cells) (2), our data suggest that photic inhibition of locomotor activity in mice is not decoded by the SCN or alternatively, that photic input to the ventral SCN is sufficient to induce this inhibition. Revealing the substrates for the exaggerated negative masking in *Scn1a*$^{+/-}$ mice may be important to understand the neural bases of hyperphotosensitivity and light-induced seizures in SMEI patients (49).

$Na_V1.1$ Channels Are Critical for SCN Interneuronal Communication. Emergent properties of the SCN neuronal network are known to be critical to produce a coherent and robust circadian output (reviewed in refs. 5 and 50). Nonspecific blockade of voltage-gated Na^+ channels with TTX desynchronizes *Per1* expression rhythms in individual SCN neurons in vitro (7). Furthermore, mathematical models clearly show that changes in coupling in a multioscillator system like the SCN can lead to changes in the emergent period of the network (51, 52), which is the case in vasoactive intestinal polypeptide (VIP) KOs; they can show periods longer or shorter than the WT period (53). Together, these findings are consistent with the altered circadian period that results from lower $Na_V1.1$ activity.

As previously reported (28, 54), light-induced expression of *Per1* in WT mice is initially restricted to the ventral SCN and later propagates to the dorsal SCN. Whereas *Scn1a*$^{+/-}$ mice showed relatively normal light-induced expression of *Per1* and *c-Fos* in the ventral SCN, expression of both genes was substantially reduced in the dorsal SCN. Furthermore, reduced $Na_V1.1$ expression leads to reduced Ca^{2+} transients in the ventral and particularly, the dorsal SCN in response to RHT stimulation. $[Ca^{2+}]_i$ increases in SCN neurons are proportional to the postsynaptic action potential frequency after excitatory postsynaptic potentials that result from RHT stimulation, but they are absent if these excitatory postsynaptic potentials fail to induce action potentials (35). Expression of both *c-Fos* and *Per1* within SCN cells is regulated by $[Ca^{2+}]_i$ (55) and action potential frequency (56). Therefore, it is likely that action potentials generated by $Na_V1.1$ channels, which are primarily localized within neuronal cell bodies and axonal hillock (19), drive entry of Ca^{2+} and expression of clock genes in the SCN and that impairment of these Ca^{2+} transients by deletion of $Na_V1.1$ channels causes the reduction of expression of *c-Fos* and *Per1*. Whereas $[Ca^{2+}]_i$ increases were reduced both in the ventral and dorsal SCNs in *Scn1a*$^{+/-}$ mice, the increase in *c-Fos* and *Per1* RNA was more severely affected in the dorsal SCN, suggesting that the $[Ca^{2+}]_i$ threshold for induction of gene expression may differ between cells of each subregion or that the action potentials

from the RHT that drive $[Ca^{2+}]_i$ increases in the ventral SCN are more robust than those action potentials that are generated in the ventral SCN and drive $[Ca^{2+}]_i$ increases in the dorsal SCN in *Scn1a*$^{+/-}$ mice.

GABAergic Transmission in the SCN Is Critical for Circadian Period Determination and Circadian Photoresponsiveness. Several studies have identified putative neurotransmitters underlying circadian coupling within the SCN neuronal network. Both GABA and VIP have been proposed as critical signals that mediate coupling of neuronal activity (5, 11, 50, 57–59). The partial rescue of the lengthened circadian period and light-induced phase shifts in *Scn1a*$^{+/-}$ mice by GABAergic transmission-enhancing drugs is consistent with a critical role of SCN GABAergic transmission in period determination and decoding of photic information. This latter role has been previously suggested by electrophysiological studies in rat brain slices using $GABA_A$ receptor antagonists, which block the ability of the ventral SCN to relay photic information to the dorsal SCN (12). Our study supports this role using both in vitro and in vivo assays in a transgenic animal model that leads to decreased GABAergic transmission. Furthermore, the pharmacological rescue of circadian abnormalities in *Scn1a*$^{+/-}$ mice that we report relies on drugs that are not $GABA_A$ receptor agonists or antagonists; instead, they enhance the effect of endogenously released GABA on this receptor.

Although GABA is predominantly an inhibitory neurotransmitter throughout the adult CNS, several studies have indicated that it can either inhibit or excite SCN neurons, and the ratio of excited/inhibited cells changes throughout the circadian cycle (12, 57, 60–62). During the circadian night, when light can phase shift the clock, a higher proportion of neurons is excited by GABA and RHT stimulation (61). After stimulation of the RHT during the subjective night, we seldom recorded inhibitory responses (i.e., decreases in $[Ca^{2+}]_i$) and mostly observed excitatory responses both in the ventral and dorsal SCNs. These excitatory responses were reduced in SCN slices from *Scn1a*$^{+/-}$ mice and dramatically decreased in slices from *Scn1a*$^{-/-}$ mice. This reduced excitability may be a consequence of decreased $Na_V1.1$ channel activity in both neurons directly innervated by RHT glutamatergic terminals as well as neurons that respond with excitatory postsynaptic potentials to GABA release from SCN interneurons.

Our results are in line with a model in which $Na_V1.1$ channel activity is critical for GABAergic neuron excitability within SCN neurons. Light during the subjective night has the ability to activate ventral SCN neurons, which in turn relay this photic information to dorsal neurons through the release of GABA. Reduced $Na_V1.1$ channel activity in *Scn1a*$^{+/-}$ mice would impair this ventral–dorsal propagation and would reduce circadian photoresponsiveness. Because VIP neurons in the SCN are GABAergic, reduced $Na_V1.1$ activity would also affect the release of this neuropeptide, further contributing to a disrupted response to light and other circadian anomalies.

SMEI and the Circadian System. Circadian abnormalities in *Scn1a*$^{+/-}$ mice derive from impaired excitability of GABAergic interneurons, which was previously observed for ataxia (14) and deficits in homeostatic regulation of sleep (63). Therefore, the comorbidities of ataxia and sleep disorders in children with SMEI may both be caused by the primary genetic defect in this disease—loss of $Na_V1.1$ channels and impairment of firing of GABAergic interneurons. Together, these results support a unified mechanism for epilepsy and comorbidities in SMEI. This fundamental pathological insight suggests that all of the symptoms of SMEI may be treatable by enhancement of GABAergic neurotransmission. The recovery of circadian abnormalities by a GABAergic transmission-enhancing diet is remarkable and suggests that similar therapies could be used to treat some of the sleep comorbidities present in SMEI patients. Of note, treatment with the combination of tiagabine and clonazepam is also effective in prevention of seizures in *Scn1a*$^{+/-}$ mice (64), and therefore, this combination therapy may indeed have value in treating both primary seizures and comorbidities of SMEI.

Methods

All experiments with animals were performed according to the National Institutes of Health Guide for Care and Use of Laboratory Animals and were approved by the University of Washington Institutional Animal Care and Use Committee.

Generation of $Na_V1.1$ Mutant Mice. Mutant mice used in this study were generated by targeted deletion of the last exon encoding domain IV from the S3 to S6 segment and the entire C-terminal tail of $Na_V1.1$ channels as described previously (13). The animals used in this study were generated by crossing heterozygous mutant males of C57BL/6 background with WT C57BL/6 females. $Na_V1.1$ null mice for calcium imaging were generated by breeding $Na_V1.1$ heterozygous pairs of mixed C57BL/6 and 129Sv background. Mice were genotyped as described previously (14).

Immunoblotting, Immunohistochemistry, and in Situ Hybridization. SCN tissue was harvested by punching the SCN regions with a 16-gauge needle from 300-μm-thick brain slices. Membrane proteins were partially purified by discontinuous sucrose gradient centrifugation, fractionated by SDS/PAGE (100 μg), and immunoblotted with an anti-$Na_V1.1$ antibody (diluted 1:200; Chemicon) as described previously (13).

In situ hybridization for the $Na_V1.1$ mRNA was performed using a digoxigenin-labeled antisense riboprobe as described before (65), with the exception that 16-μm coronal sections were cut from fresh-frozen brains. The probe was generated from an *Scn1a* PCR-specific product (forward primer containing T3 promoter: 5′-AATTAACCCTCACTAAAGGGCATTCAGCGAGCTTATAGGCGCCACC-3′; reverse primer containing T7 promoter: 5′-TAATACGACTCACTATAGGGCACAGGCTGTAAACAATTTG TCACCCA-3′). *Scn1a* signal was detected using antidigoxigenin antibody (diluted 1:200; Roche). For double-labeling experiments, monoclonal anti-GAD67 (diluted 1:200; Chemicon) was added at the same time as antidigoxigenin antibody. For controls, the primary antiserum was omitted or replaced with normal rabbit serum. In situ hybridization for *c-Fos*, *mPer1*, and *mPer2* was performed with radiolabeled riboprobes as previously described (65). Autoradiographic images were generated by exposing slides to Ultramax film (Kodak). Images were scanned at high resolution, and hybridization intensities were determined with ImageJ software (National Institutes of Health) using templates for the whole SCN (Fig. 5) or the ventral and dorsal SCNs (Fig. 6).

Behavioral Measurements and Analysis. Adult *Scn1a*$^{+/-}$ mice and their WT littermates were housed in individual cages equipped with a running wheel and maintained in ventilated, light-tight chambers. Wheel-running activity was monitored in 10-min bins using Clocklab software (Actimetrics) and analyzed using the El Temps software (Diéz-Noguera, University of Barcelona, Barcelona, Spain). Animals were entrained to a 12:12 LD cycle (lights on 8:00 AM) with 200-lux intensity for at least 14 d before release into constant DD. Free-running period was measured using periodogram analysis (66). To determine the light-induced phase shift of locomotor activity, animals in their home cages were moved to another chamber and exposed to a 30-min pulse of white light (500 lux) at CT16; dark-treated controls were moved but received no light treatment. Because light acutely inhibits wheel-running activity, the analysis of reentrainment rate after abrupt shifts of the LD cycles was different for advances and delays. For advances, the number of days for the onset of activity to reach its original phase relationship with the LD cycle was counted. For delays, the number of days for the offset of activity to reach its original phase relationship was counted. For all phase-shifting stimuli, no cage changes were scheduled on the days after the stimulus, because cage changes are known to induce phase shifts. Waveforms were calculated by first calculating the 10-min mean of wheel-running activity for several successive days for each animal; then, the mean ± SEM was calculated for all of the animals for each 10- (Fig. 8*B*) or 30-min (Fig. 2*D*) interval. Phase angle of entrainment was calculated by estimating the difference in minutes between the activity onset on the first day after release into DD and the extrapolated time of lights off (from the previous day) to discard the effects of negative masking by light.

ERG. ERG was performed using a Ganzfeld bowl, direct current amplifier, and PC-based control and recording system (Multiliner Vision; VIASYS Healthcare

GmbH). Mice were dark-adapted overnight and anesthetized with ketamine (67 mg/kg) and xylazine (12 mg/kg). Pupils were dilated with tropicamide. Single-flash 1.5-log cd × s/m^2 stimuli were delivered under dark-adapted conditions. ERG responses were recorded under the intensity that led to maximum amplitude response in both WT and *Scn1a*$^{+/-}$ mice (1.5 log cd × s/m^2). Ten responses were averaged, with an interstimulus interval of 17 s.

Calcium Imaging. For $[Ca^{2+}]_i$ imaging experiments, SCN slices from P15 to P20 mice were prepared during the early subjective night (ZT14 to -15) and maintained in artificial cerebrospinal fluid containing 1.75 μM of the $[Ca^{2+}]_i$ indicator dye fluo-4 and 0.07% Pluronic-127 (Molecular Probes/Invitrogen) for 20 min as previously described (67). After loading, the tissue was positioned in a microscope chamber and imaged on a Nikon inverted Diaphot microscope with a cooled CCD camera (Photometrics) at 3 Hz. The chamber was constantly perfused with carbogen-bubbled ACSF at a rate of 1 mL min^{-1}. Images and measurements were recorded using MetaFluor (Universal Imaging/Molecular Devices) and subsequently analyzed using MetaFluor Analyst, SigmaPlot (Systat), Microsoft Excel 2007, ImageJ (National Institutes of Health), and Adobe Photoshop. The gradual baseline decline in $[Ca^{2+}]_i$ imaging traces is caused by photobleaching. The RHT was stimulated by a concentric bipolar electrode placed in the optic chiasm about 200 μm from the SCN at the indicated frequency for 2 s. At the end of each experiment, the slice was stimulated by application of 1 mM glutamate to confirm a similar response by fluo-4–imaged cells, which suggests that recorded cells were neurons and not glial cells; glial cells do not show transient $[Ca^{2+}]_i$ changes in response to glutamate.

Statistical Analysis. Data are presented as mean ± SEM (one- or two-way ANOVA followed by Tukey or Student *t* contrasts for comparisons in which type I error was not possible). $P < 0.05$ was considered as statistically significant. Statistical analysis was done using the JMP software.

ACKNOWLEDGMENTS. This work was supported by US National Institutes of Health Research Grants R01 NS25704 (to W.A.C.) and R01 MH075016 (to H.O.d.l.l.) and Core Grant for Vision Research Grant P30EY1730.

1. Hastings MH, Reddy AB, Maywood ES (2003) A clockwork web: Circadian timing in brain and periphery, in health and disease. *Nat Rev Neurosci* 4:649–661.
2. Morin LP, Allen CN (2006) The circadian visual system, 2005. *Brain Res Brain Res Rev* 51:1–60.
3. Welsh DK, Logothetis DE, Meister M, Reppert SM (1995) Individual neurons dissociated from rat suprachiasmatic nucleus express independently phased circadian firing rhythms. *Neuron* 14:697–706.
4. Reppert SM, Weaver DR (2001) Molecular analysis of mammalian circadian rhythms. *Annu Rev Physiol* 63:647–676.
5. Welsh DK, Takahashi JS, Kay SA (2010) Suprachiasmatic nucleus: Cell autonomy and network properties. *Annu Rev Physiol* 72:551–577.
6. Colwell CS (2011) Linking neural activity and molecular oscillations in the SCN. *Nat Rev Neurosci* 12:553–569.
7. Yamaguchi S, et al. (2003) Synchronization of cellular clocks in the suprachiasmatic nucleus. *Science* 302:1408–1412.
8. Abrahamson EE, Moore RY (2001) Suprachiasmatic nucleus in the mouse: Retinal innervation, intrinsic organization and efferent projections. *Brain Res* 916:172–191.
9. Moore RY, Speh JC (1993) GABA is the principal neurotransmitter of the circadian system. *Neurosci Lett* 150:112–116.
10. O'Hara BF, Andretic R, Heller HC, Carter DB, Kilduff TS (1995) GABAA, GABAC, and NMDA receptor subunit expression in the suprachiasmatic nucleus and other brain regions. *Brain Res Mol Brain Res* 28:239–250.
11. Liu C, Reppert SM (2000) GABA synchronizes clock cells within the suprachiasmatic circadian clock. *Neuron* 25:123–128.
12. Albus H, Vansteensel MJ, Michel S, Block GD, Meijer JH (2005) A GABAergic mechanism is necessary for coupling dissociable ventral and dorsal regional oscillators within the circadian clock. *Curr Biol* 15:886–893.
13. Yu FH, et al. (2006) Reduced sodium current in GABAergic interneurons in a mouse model of severe myoclonic epilepsy in infancy. *Nat Neurosci* 9:1142–1149.
14. Kalume F, Yu FH, Westenbroek RE, Scheuer T, Catterall WA (2007) Reduced sodium current in Purkinje neurons from Nav1.1 mutant mice: Implications for ataxia in severe myoclonic epilepsy in infancy. *J Neurosci* 27:11065–11074.
15. Claes L, et al. (2001) De novo mutations in the sodium-channel gene SCN1A cause severe myoclonic epilepsy of infancy. *Am J Hum Genet* 68:1327–1332.
16. Wolff M, Cassé-Perrot C, Dravet C (2006) Severe myoclonic epilepsy of infants (Dravet syndrome): Natural history and neuropsychological findings. *Epilepsia* 47(Suppl 2): 45–48.
17. Wallace RH, et al. (2003) Sodium channel alpha1-subunit mutations in severe myoclonic epilepsy of infancy and infantile spasms. *Neurology* 61:765–769.
18. Catterall WA, Kalume F, Oakley JC (2010) $Na_V1.1$ channels and epilepsy. *J Physiol* 588: 1849–1859.
19. Westenbroek RE, Merrick DK, Catterall WA (1989) Differential subcellular localization of the RI and RII Na^+ channel subtypes in central neurons. *Neuron* 3:695–704.
20. Daan S, Aschoff J (2001) *The Entrainment of Circadian Systems. Handbook of Behavioral Neurobiology: Circadian Clocks*, eds Takahashi JS, Turek F (Kluwer, Boston), Vol 12, pp 7–42.
21. Johnson CH, Elliott JA, Foster R (2003) Entrainment of circadian programs. *Chronobiol Int* 20:741–774.
22. Schwartz WJ, Zimmerman P (1990) Circadian timekeeping in BALB/c and C57BL/6 inbred mouse strains. *J Neurosci* 10:3685–3694.
23. Mrosovsky N (1999) Masking: History, definitions, and measurement. *Chronobiol Int* 16:415–429.
24. Tei H, et al. (1997) Circadian oscillation of a mammalian homologue of the Drosophila period gene. *Nature* 389:512–516.
25. Sun ZS, et al. (1997) RIGUI, a putative mammalian ortholog of the Drosophila period gene. *Cell* 90:1003–1011.
26. Shearman LP, Zylka MJ, Weaver DR, Kolakowski LF, Jr., Reppert SM (1997) Two period homologs: Circadian expression and photic regulation in the suprachiasmatic nuclei. *Neuron* 19:1261–1269.
27. Kornhauser JM, Nelson DE, Mayo KE, Takahashi JS (1990) Photic and circadian regulation of c-fos gene expression in the hamster suprachiasmatic nucleus. *Neuron* 5: 127–134.
28. Shigeyoshi Y, et al. (1997) Light-induced resetting of a mammalian circadian clock is associated with rapid induction of the mPer1 transcript. *Cell* 91:1043–1053.
29. de la Iglesia HO, Cambras T, Schwartz WJ, Díez-Noguera A (2004) Forced desynchronization of dual circadian oscillators within the rat suprachiasmatic nucleus. *Curr Biol* 14:796–800.
30. Schwartz MD, Congdon S, de la Iglesia HO (2010) Phase misalignment between suprachiasmatic neuronal oscillators impairs photic behavioral phase shifts but not photic induction of gene expression. *J Neurosci* 30:13150–13156.
31. Schwartz MD, et al. (2009) Dissociation of circadian and light inhibition of melatonin release through forced desynchronization in the rat. *Proc Natl Acad Sci USA* 106: 17540–17545.
32. Nakamura W, Yamazaki S, Takasu NN, Mishima K, Block GD (2005) Differential response of Period 1 expression within the suprachiasmatic nucleus. *J Neurosci* 25: 5481–5487.
33. Hannibal J (2002) Neurotransmitters of the retino-hypothalamic tract. *Cell Tissue Res* 309:73–88.
34. Golombek DA, Rosenstein RE (2010) Physiology of circadian entrainment. *Physiol Rev* 90:1063–1102.
35. Irwin RP, Allen CN (2007) Calcium response to retinohypothalamic tract synaptic transmission in suprachiasmatic nucleus neurons. *J Neurosci* 27:11748–11757.
36. Berson DM, Dunn FA, Takao M (2002) Phototransduction by retinal ganglion cells that set the circadian clock. *Science* 295:1070–1073.
37. Bachmanov AA, Reed DR, Beauchamp GK, Tordoff MG (2002) Food intake, water intake, and drinking spout side preference of 28 mouse strains. *Behav Genet* 32: 435–443.
38. Vitaterna MH, et al. (1994) Mutagenesis and mapping of a mouse gene, Clock, essential for circadian behavior. *Science* 264:719–725.
39. Nolan KJ, Camfield CS, Camfield PR (2006) Coping with Dravet syndrome: Parental experiences with a catastrophic epilepsy. *Dev Med Child Neurol* 48:761–765.
40. Toh KL, et al. (2001) An hPer2 phosphorylation site mutation in familial advanced sleep phase syndrome. *Science* 291:1040–1043.
41. Xu Y, et al. (2007) Modeling of a human circadian mutation yields insights into clock regulation by PER2. *Cell* 128:59–70.
42. VanderLeest HT, Rohling JH, Michel S, Meijer JH (2009) Phase shifting capacity of the circadian pacemaker determined by the SCN neuronal network organization. *PLoS One* 4:e4976.
43. VanderLeest HT, et al. (2007) Seasonal encoding by the circadian pacemaker of the SCN. *Curr Biol* 17:468–473.
44. Baba K, Ono D, Honma S, Honma K (2008) A TTX-sensitive local circuit is involved in the expression of PK2 and BDNF circadian rhythms in the mouse suprachiasmatic nucleus. *Eur J Neurosci* 27:909–916.
45. Kudo T, Loh DH, Kuljis D, Constance C, Colwell CS (2011) Fast delayed rectifier potassium current: Critical for input and output of the circadian system. *J Neurosci* 31: 2746–2755.
46. Nakamura TJ, et al. (2011) Age-related decline in circadian output. *J Neurosci* 31: 10201–10205.
47. Mrosovsky N, Hattar S (2003) Impaired masking responses to light in melanopsin-knockout mice. *Chronobiol Int* 20:989–999.
48. Hannibal J, Brabet P, Fahrenkrug J (2008) Mice lacking the PACAP type I receptor have impaired photic entrainment and negative masking. *Am J Physiol Regul Integr Comp Physiol* 295:R2050–R2058.
49. Guerrini R, Genton P (2004) Epileptic syndromes and visually induced seizures. *Epilepsia* 45(Suppl 1):14–18.
50. Aton SJ, Herzog ED (2005) Come together, right. . .now: Synchronization of rhythms in a mammalian circadian clock. *Neuron* 48:531–534.
51. Daan S, Berde C (1978) Two coupled oscillators: Simulations of the circadian pacemaker in mammalian activity rhythms. *J Theor Biol* 70:297–313.
52. Bernard S, Gonze D, Cajavec B, Herzel H, Kramer A (2007) Synchronization-induced rhythmicity of circadian oscillators in the suprachiasmatic nucleus. *PLoS Comput Biol* 3:e68.

53. Aton SJ, Colwell CS, Harmar AJ, Waschek J, Herzog ED (2005) Vasoactive intestinal polypeptide mediates circadian rhythmicity and synchrony in mammalian clock neurons. *Nat Neurosci* 8:476–483.
54. Albrecht U, Sun ZS, Eichele G, Lee CC (1997) A differential response of two putative mammalian circadian regulators, mper1 and mper2, to light. *Cell* 91:1055–1064.
55. Yokota S, et al. (2001) Involvement of calcium-calmodulin protein kinase but not mitogen-activated protein kinase in light-induced phase delays and Per gene expression in the suprachiasmatic nucleus of the hamster. *J Neurochem* 77:618–627.
56. Kuhlman SJ, Silver R, Le Sauter J, Bult-Ito A, McMahon DG (2003) Phase resetting light pulses induce Per1 and persistent spike activity in a subpopulation of biological clock neurons. *J Neurosci* 23:1441–1450.
57. Wagner S, Yarom Y (2009) Excitation by GABA in the SCN reaches its time and place (Commentary on Irwin & Allen). *Eur J Neurosci* 30:1461.
58. Harmar AJ, et al. (2002) The VPAC(2) receptor is essential for circadian function in the mouse suprachiasmatic nuclei. *Cell* 109:497–508.
59. Maywood ES, Chesham JE, O'Brien JA, Hastings MH (2011) A diversity of paracrine signals sustains molecular circadian cycling in suprachiasmatic nucleus circuits. *Proc Natl Acad Sci USA* 108:14306–14311.
60. Wagner S, Castel M, Gainer H, Yarom Y (1997) GABA in the mammalian suprachiasmatic nucleus and its role in diurnal rhythmicity. *Nature* 387:598–603.
61. Irwin RP, Allen CN (2009) GABAergic signaling induces divergent neuronal Ca^{2+} responses in the suprachiasmatic nucleus network. *Eur J Neurosci* 30:1462–1475.
62. Choi HJ, et al. (2008) Excitatory actions of GABA in the suprachiasmatic nucleus. *J Neurosci* 28:5450–5459.
63. Kalume F, Oakley JC, Westenbroek RE, Scheuer T, Catterall WA (2010) Reduced excitability of GABAergic interneurons in the reticular nucleus of the thalamus and sleep impairment in a mouse model of Severe Myoclonic Epilepsy of Infancy. *Soc Neurosci Abs*15.
64. Oakley JC, Kalume F, Catterall WA (2011) Insights into pathophysiology and therapy from a mouse model of Dravet syndrome. *Epilepsia* 52(Suppl 2):59–61.
65. de la Iglesia HO (2007) In situ hybridization of suprachiasmatic nucleus slices. *Methods Mol Biol* 362:513–531.
66. Sokolove PG, Bushell WN (1978) The chi square periodogram: Its utility for analysis of circadian rhythms. *J Theor Biol* 72:131–160.
67. Moruzzi AM, Abedini NC, Hansen MA, Olson JE, Bosma MM (2009) Differential expression of membrane conductances underlies spontaneous event initiation by rostral midline neurons in the embryonic mouse hindbrain. *J Physiol* 587:5081–5093.